DNA-Binding Interactions and Conformational Fluctuations of Tc3 Transposase DNA Binding Domain Examined with Single Molecule Fluorescence Spectroscopy

Douglas C. Daniel, Martin Thompson, and Neal W. Woodbury

Department of Chemistry and Biochemistry, Arizona State University, Tempe, Arizona 85287-1604 USA

ABSTRACT The fluorescent dye tetramethylrhodamine (TMR) was conjugated to a synthetic peptide containing the sequence-specific DNA binding domain of Tc3 transposase. Steady-state and single molecule fluorescence spectroscopy was used to investigate protein conformational fluctuations and the thermodynamics of binding interactions. Evidence is presented to show that the TMR-Tc3 conjugate exists in at least two conformational states. The most stable conformation is one in which the TMR fluorescence is quenched. Upon binding to DNA, the total fluorescence from TMR-Tc3 increases by three- to fourfold. Single molecule measurements of TMR-Tc3 bound to DNA shows that this complex also fluctuates between a fluorescent and quenched form. The fluorescent form of the conjugate is stabilized when bound to DNA, and this accounts for part of the increase in total fluorescence. In addition, the inherent photodynamics of the dye itself is also altered (e.g., fluorescent lifetime or triplet yield) in such a way that the total fluorescence from the conjugate bound to DNA is enhanced relative to the unbound form.

INTRODUCTION

Proteins that recognize and bind specific DNA sequences are ubiquitous in biological systems and serve to perform a variety of functions critical to the survival of cellular organisms. DNA repair, replication, recombination, transcription, and gene regulation are all mediated by sequence specific DNA binding proteins (Burley, 1996; Krajewska, 1992; Walther et al., 1999). Current conceptual models of such interactions are derived almost exclusively from population averaged data. However, the relevant molecular interactions and chemical reactions that govern these processes are usually described from a single molecule viewpoint. As a result, biological processes are typically portrayed as proceeding stepwise through a series of sequential events that transform the system from an initial state to some final state. Each mechanistic step is considered to convert the system from one thermodynamically static state to another. This thought process leads to a static picture of binding or conformation. A transcription factor, for example, is generally envisaged as binding to DNA, changing conformation or effecting a conformational change in some other component of the translational machinery, and when its function is complete, dissociating. However, this simple conceptual model is an incomplete description.

Notwithstanding the fact that population averaged properties remain constant, from a molecular point of view, there is clearly a dynamical aspect of chemical equilibrium to consider. Proteins actively bind and dissociate from their target sequences in a perpetual manner. Conformational changes are also dynamic, taking place both in free form and when associated with other macromolecules. Also, fluctuations of the spectroscopic state of a molecule occur continuously and spontaneously. These temporal fluctuations generally cannot be resolved in ensemble averaged measurements, unless the system data are obtained by monitoring the concerted evolution of a molecular ensemble that is far from equilibrium. Moreover, bulk phase measurements are blind to the distribution of most molecular properties because only average values are accessible. For example, a 30% change in enzymatic activity, as measured in a population averaged experiment, could arise either from a fractional but homogeneous change in the activity of all the enzymes comprising the population, or it could result from a shift in the relative number of enzyme molecules in an active versus inactive conformation at any given time. In the latter case the observed increase in activity is due to a shift in equilibrium between members of an inhomogeneous population.

Recent advances in fluorescence correlation spectroscopy (FCS) and single molecule spectroscopic techniques have made it possible to examine equilibrium systems and record real-time fluctuations in fluorescence emission from individual molecules, complexes, or aggregates. From these types of measurements dynamic information and details of the distribution of species within the sample, even at equilibrium, can be extracted. Single molecule spectroscopy allows one to follow the trajectory of a molecular property in real time and is particularly suited to monitoring fluctuations that occur on the 100 μs to 10 ms timescale. Analysis of long-term fluctuations is limited by photobleaching, whereas analysis of sub-microsecond timescale fluctuations is restricted by the limited density of collected photons from an individual

Submitted June 18, 2001 and accepted for publication November 19, 2001.

Address reprint requests to Dr. Neal Woodbury, Arizona State University, Department of Chemistry and Biochemistry, Tempe, AZ 85287-1604. Tel.: 480-965-3294; Fax: 480-965-2747; E-mail: nwoodbury@asu.edu.

0006-3495/02/03/1654/13 $2.00

molecule. A direct recording of these fluorescence fluctuations contains information unavailable from bulk spectroscopy.

The potential of single molecule fluorescence spectroscopy to provide solutions to real biological problems that cannot be obtained from traditional bulk measurements is for the most part still unrealized, but the field is young. Potential applications have been recognized, and substantial progress has been made in the development of instrumentation and procedures for manipulating and measuring individual molecules. Single molecule experiments have been performed and validated by comparison to bulk data, although, most of these measurements have been made on relatively simple systems (Deniz et al., 2000; Eggeling et al., 1998, 2001; Ha et al., 1999a,b; Lu and Xie, 1997; Zander et al., 1996). Contributing to the difficulty of making the transition from novel spectroscopy to problem solving is that with the additional information available at the single molecule level, even relatively simple systems (such as a dye molecule attached to DNA) show rather complex behavior, due to the fact that at the single molecule level all of the conformational and chemical inhomogeneity becomes visible. Thus, it has been necessary initially to work with well-defined and relatively simple biological systems to develop the analytical methodology required to determine what aspects of the observed dynamics have biological relevance. Our laboratory has synthesized a variety of small DNA-binding domains with associated dye probes and characterized their interactions with DNA in the bulk phase in detail. This work was done in preparation for measurements at the single molecule level using well-characterized systems. One such system is the DNA binding domain of the transposase Tc3 of *Caenorhabditis elegans* (van Pouderoyen et al., 1997). In previous work, this domain was synthesized, and the binding was characterized as a function of various parameters (Thompson and Woodbury, 2000). In this study, a version of that domain was specifically synthesized with a fluorophore that would not interfere with the DNA binding but would report on the changes in its environment. It is shown that this fluorophore is indeed sensitive to conformational changes induced upon DNA binding (the fluorescence level increases three- to fourfold). Single molecule spectroscopy is used to approach the question of whether this is a homogeneous change in conformation or a shift in the equilibrium between two conformational states. Comparison of the single molecule properties on the time scales for binding, diffusion, and conformational interconversion reveals a shift in conformational dynamics on the millisecond timescale between the bound and unbound forms.

Tc3 of *C. elegans* functions as a transposase, removing a small section of DNA and transferring it from one place in the genome to another. The particular protein used in this study is a 52 residue fragment that includes the DNA binding domain. The peptide derives from residues 202 to 253 of the native Tc3. This portion of the peptide contains a helix-turn-helix DNA binding motif that binds the major groove of DNA. Data from x-ray crystallography have shown that the N terminus of the peptide sits in the minor groove and thus adds further stabilization to the binding interaction. Fig. 1 shows the geometry of the binding interaction and peptide secondary structure as obtained from the Protein Database Bank (ID: 1Tc3). To this DNA binding domain a fluorescent dye, tetramethylrhodamine (TMR), was attached so that its behavior could be monitored. Fluorescence anisotropy measurements show that that the dye labeled peptide retained its ability to recognize and bind to its native DNA sequence (see Results).

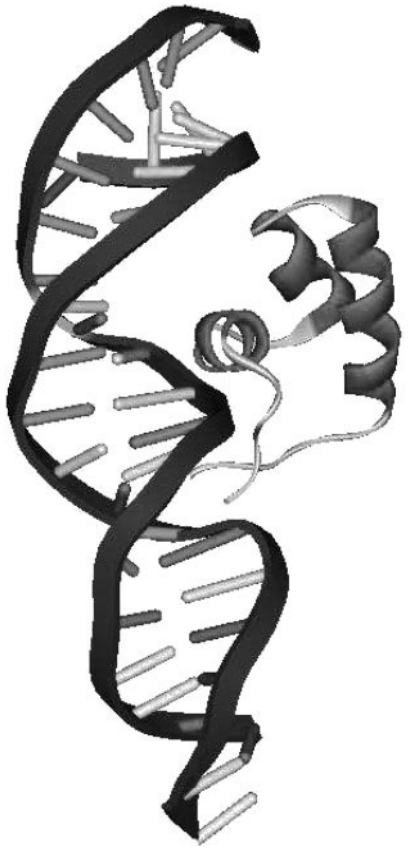

FIGURE 1 Geometry of Tc3 binding to its native DNA binding domain as obtained from the Protein Data Bank and identified with the PDB ID: 1Tc3. The TMR label, not shown, was attached to lysine residue 210 so that it was positioned away from the binding site.

MATERIALS AND METHODS

Apparatus

Fig. 2 shows a schematic drawing of the experimental setup for fluorescence detection of single molecules. The arrange-

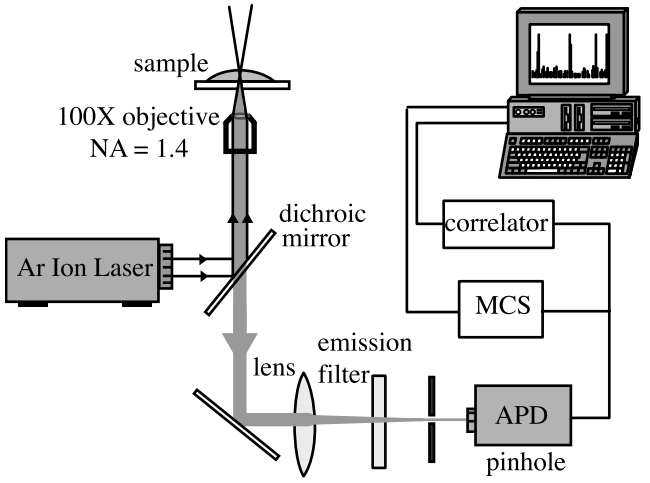

FIGURE 2 Experimental setup for collection of MCS and ACF data.

ment is similar to that described previously (Daniel et al., 2000). Briefly, the sample is excited in the confocal spot of a high numerical aperture objective (Nikon 100×, N.A. = 1.4) with the 514-nm line of an argon ion laser. Fluorescence passes through a 100-μm confocal pinhole to reject out of focus light and is subsequently imaged onto an avalanche photodiode (SPCM-AQ-151, EG&G, Vaudreuil, Quebec, Canada) operating in single photon counting mode. Signal from the APD was split and directed to two data acquisition devices. A multichannel scaler (MCS-plus, EG&G) was used to record temporal fluctuations in fluorescence from individual fluorescent species freely diffusing in the open probe volume. The MCS card counted photons and binned them into preset time intervals. A real-time digital correlator card (Flex2K-12X2, correlator.com) was used to obtain fluorescence intensity autocorrelation functions. All measurements reported were performed with fresh solutions prepared by serial dilution of the stock in buffer. Steady-state fluorescence and fluorescence anisotropy measurements were performed on a SPEX Fluorolog-2 fluorometer.

Reagents and chemicals

Oligonucleotides were purchased from Sigma-Genosys (The Woodlands, TX) and further purified on a 15% denaturing polyacrylamide gel. Bands were excised from the gel and the nucleic acid material extracted by soaking crushed gel pieces in 100 mM Tris, (pH 8.0) 100 mM NaCl buffer overnight. A size exclusion column packed with Sephadex G-15 resin was used to remove urea and excess salt. Final purification was achieved through chloroform extraction using spectroscopic grade solvent (Aldrich, St. Louis, MO). Annealed ds-DNA was prepared by heating equimolar amounts of complimentary single strands to 90°C for 2 to 3 min and slowly cooling to room temperature. Final concentrations were verified by measuring the absorbance at 260 nm. For all MCS and FCS experiments a 32-base nucleotide (DNA_{BD}) was used having the sequence 5′-TCG-GCACGCTGCTAGTTCTATAGGACCCC CC -3′. The DNA used for steady-state experiments was composed of 40 bp having the sequence 5′-GCTGACTGCG TTCTATAG-GACCCCCCCGCTGACTGCATCA-3′. The underlined bases indicate the Tc3 binding domain. Although the sequence outside the binding region differs somewhat between the oligonucleotides used for the single molecule versus the bulk phase studies, this should not significantly affect the conformational change and associated fluorescence change of the TMR-Tc3 upon binding to its specific sequence.

The tetramethyl rhodamine labeled Tc3 (TMR-Tc3) was synthesized on 5-(4′-Fmoc-aminomethyl-3′,5′dimethoxy-phenoxy)valeric acid polyethylene glycol polystyrene resin by automated solid-phase peptide synthesis using F-moc chemistry analogous to the synthesis by Thompson and Woodbury (2000) of thiazole orange labeled Tc3. The sequenced peptide derives from residues 202 to 253 of the native Tc3 with residue 210 (threonine) replaced by a lysine to which the dye was subsequently attached. This attachment positioned the dye away from the peptide-DNA binding site and thus prevented direct interactions between DNA and TMR that could otherwise strongly perturb the fluorescence properties of the dye and possibly to the peptide/DNA interactions (Vámosi et al., 1996). The peptide was purified by reverse phase-high performance liquid chromatography on a Zorbax C8 using a water (0.1% tetrafluoroacetic acid) to acetonitrile (0.1% TFA) gradient. The identity of the peptide was confirmed by amino acid analysis and matrix-assisted laser desorption ionization-time-of-flight (MALDI-TOF). Peptide quantification was achieved using the Bradford Assay with a bovine serum albumin reference (Bradford, 1976).

Oligonucleotides and peptide samples were stored frozen in buffer at −20°C. Throughout the paper the term "buffer" refers to 10 mM trizma base, 20 mM NaCl, and 700 μM $MgCl_2$ adjusted to pH 7.5 with HCl. The water used in all samples was double distilled, passed through a Millipore filtration system, and sterilized by autoclaving.

RESULTS

Steady-state fluorescence spectroscopy

Upon addition of DNA_{BD} to TMR-Tc3 a substantial increase in the total fluorescence amplitude was observed. Fig. 3 displays the bulk phase emission spectra (λ_{exc} = 520 nm) obtained from TMR-Tc3 in the presence and absence of the DNA binding domain. A fourfold increase in the fluorescence from the system is evident when DNA containing the binding site is present. From this, one might suppose that binding induces a conformational change in the protein

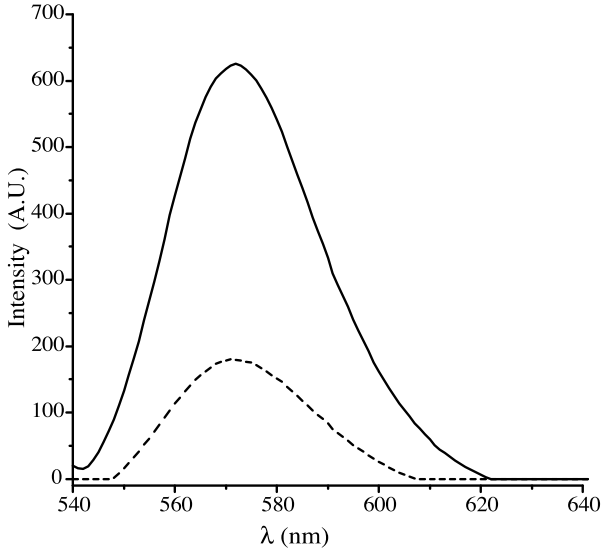

FIGURE 3 Emission spectra of TMR-Tc3 with (*solid*) and without (*dashed*) DNA (λ_{exc} = 520 nm). Spectra were acquired in pH 7.8 buffer, 10 mM trizma base, 100 mM NaCl. The 40-bp DNA sequence used for these measurements with the Tc3 binding site underlined is: 5′-GCTGACTGCGTTCTATAGGACCCCCCCGCTGACTGCATCA-3′. Both protein and DNA were at 50 nM concentration.

that favors a less quenched state. There are many examples in biology in which a protein binds DNA and changes conformation (Jäger and Pata, 1999; Schildbach et al., 1999; Soultanas et al., 1999). This particular system has a covalently linked fluorescent probe, which allows one to monitor these conformational changes spectroscopically.

Fig. 4 shows the results from fluorescence anisotropy

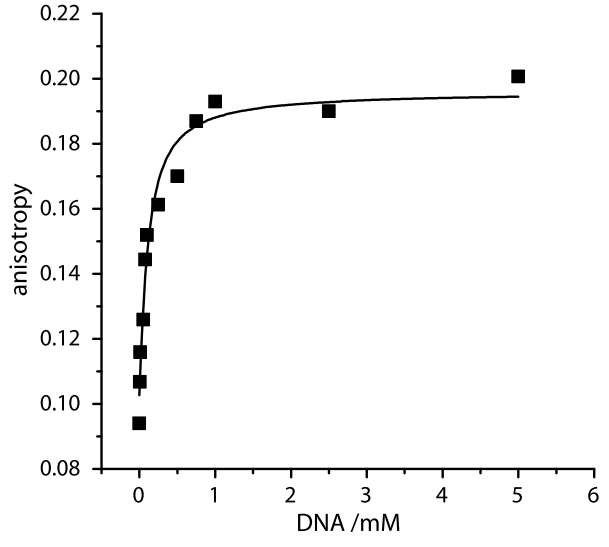

FIGURE 4 Fluorescence anisotropy of 10 nM TMR-Tc3 versus amount DNA (nM) added to solution. The measured data points (*circles*) were fit using a two-state model (*solid curve*) in which the protein was either bound or unbound (see text). The titrated DNA is the same as that for Fig. 3.

experiments that were conducted to determine the dissociation constant, K_D, of TMR-Tc3 with its native consensus site. The fluorescence anisotropy of a 50 nM TMR-Tc3 solution was measured as a function of added unlabeled DNA containing the Tc3 binding site. A two-state model was assumed in which the protein was either bound or unbound so that the data could be fit to the equation below (Thompson and Woodbury, 2000).

$$A = A_f + \frac{(A_b - A_f)}{2[T]_{tot}}([D]_{tot} + [T]_{tot} + K_D - (([D]_{tot} + K_D - [T]_{tot})^2 + 4K_D[T]_{tot})^{1/2}) \quad (1)$$

A_f and A_b are the anisotropies of the free and bound Tc3 respectively, and $[D]_{tot}$ and $[T]_{tot}$ are the total concentrations of DNA and TMR-Tc3. The anisotropies were defined as $A = (I_{\|} - gI_{\perp})/(I_{\|} + 2gI_{\perp})$ with $I_{\|}$ and $I_{\perp}$ representing respectively the intensities of the emission polarized parallel or orthogonal to the excitation source. The g factor corrects for any biasing in collection efficiency for the $I_{\|}$ versus $I_{\perp}$ channels. Anisotropy data were fitted to Eq. 1 using a nonlinear least squares algorithm, and K_D was determined to be 86 nM for the TMR-Tc3. The K_D for the unlabeled Tc3, determined to be 80 nM, was found similarly by titrating the unlabeled peptide with TMR labeled DNA having the consensus site. In addition, previous studies have shown that Tc3 binds to a nonspecific sequence with a 60-fold lower affinity than it does to its native consensus sequence (Thompson and Woodbury 2001). Thus, the dye label has little effect on the binding affinity of the protein to DNA_{BD}, presumably due to its remote location relative to the DNA binding surface of the peptide. For the concentrations used in the experiments described below (1 nM Tc3 and 2 μM DNA_{BD}), the protein should be bound to DNA_{BD} over 95% of the time and essentially exclusively to its native consensus site.

Fluorescence correlation spectroscopy

In a typical FCS experiment the autocorrelation function (ACF) of the fluorescence intensity of molecules diffusing through a small volume element (0.2–100 fl) is computed. The ACF decays from an initial value of $\langle I^2 \rangle$ to a final value of $\langle I \rangle^2$, in which the angle brackets represent an ensemble average. The rate and shape of this decay is a function of fluorophore concentration, size of the volume element, and the kinetic parameters of any process causing the fluorescence intensity to deviate from its mean value. In essence, the ACF describes the average duration over which fluorescence intensity fluctuations are persistent. The normalized fluorescence intensity ACF at delay time τ may be expressed as $G_n(\tau) = \langle I(t)I(t + \tau)\rangle/\langle I(t)\rangle^{-2}$. FCS was used here to determine the size of the detection volume in the confocal microscope setup. This goal was accomplished by calculat-

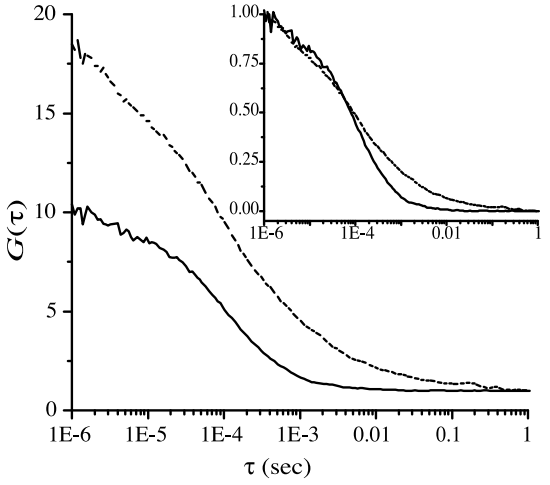

FIGURE 5 ACF for 1 nM TMR-Tc3 with (*dashed*) and without (*solid*) DNA_{BD}. Inset shows amplitude normalized ACF. Excitation power equal to 600 μW.

ing the ACF for solutions of both TMR and R6G (rhodamine 6G) in water (data not shown) and fitting the function to a model that describes freely diffusing particles through a Gaussian shaped volume element. The diffusion model is given by Rigler and others (1993)

$$G_n(\tau) = 1 + \frac{1}{\langle N\rangle}\left(1 + \frac{4D\tau}{w_0^2}\right)^{-1}\left(1 + \frac{4D\tau}{z_0^2}\right)^{-1/2} \quad (2)$$

in which $\langle N\rangle$ is the average number of fluorophores within the probe volume and D is the diffusion coefficient. The dimensions of the probe volume are given by w_0 and z_0, which represent the point where the laser beam intensity has dropped by $1/e^2$ of its maximum in the radial and axial directions, respectively. The ACF was fit to Eq. 2 using a least squares algorithm and assuming a diffusion constant of 2.8×10^{-6} cm^2 s^{-1}. The two dyes yielded nearly identical values of $w_0 = 0.31 \pm 0.01$ μm and $z_0 = 9.8 \pm 0.3$ μm with incident laser intensities of 600 and 300 μW for TMR and R6G, respectively. The probe volume, approximated as a cylinder, is given by $V = \pi w_0^2(2z_0)$. Using the dimensions above, the calculated probe volume, V_p, is found to be 3.0 ± 0.2 fl.

FCS was also used to qualitatively assess the binding interactions of TMR-Tc3 with DNA_{BD}. Autocorrelation data for TMR-Tc3 both with and without the addition of the oligonucleotide are shown in Fig. 5. It is clear that the autocorrelation curve for TMR-Tc3 alone decays faster than the one for TMR-Tc3 and DNA_{BD} together. This result is consistent with binding of the TMR-Tc3 to the DNA_{BD}, although further analysis below suggests that the decay of the autocorrelation function is not diffusion limited.

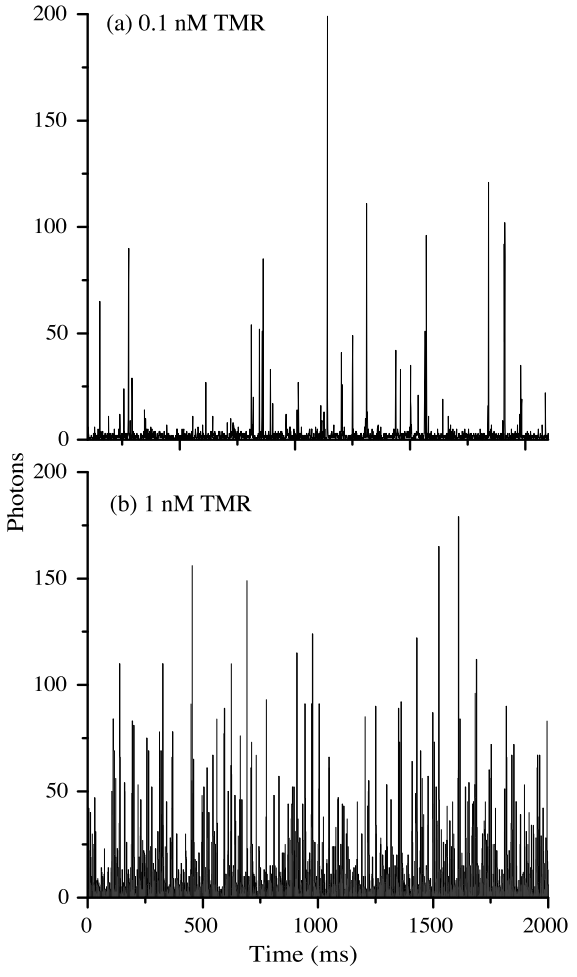

FIGURE 6 MCS data for (*a*) 0.1 nM TMR; (*b*) 1 nM TMR in water with 1-ms integration.

Single molecule MCS data

One condition for observing fluorescence from single molecules diffusing in solution is that the sample must be sufficiently dilute and the volume of observation sufficiently small such that on the average there is less than one molecule in the probe volume at any given time. The probability, P_m, of there being m molecules in probe volume is calculated from Poisson statistics (Kingman, 1993).

$$P_m = \frac{\langle N\rangle^m}{m!}\exp(-\langle N\rangle) \quad (3)$$

$\langle N\rangle = [C]V_p \times 6.023 \times 10^{23}$ is the average number of fluorophores within the probe volume (3.0 fl), and [C] is the concentration. Thus, for a probe volume of 3.0 fl to have the average number of analyte molecules ≤ 1 the concentration must be $\leq 5.5 \times 10^{-10}$ M. At 1 nM concentration, $\langle N\rangle = 1.8$, and the probe volume is unoccupied 17% of the time and contains one and two analyte molecules 30% and 27% of the time, respectively. At 0.1 nM concentration, $\langle N\rangle =$

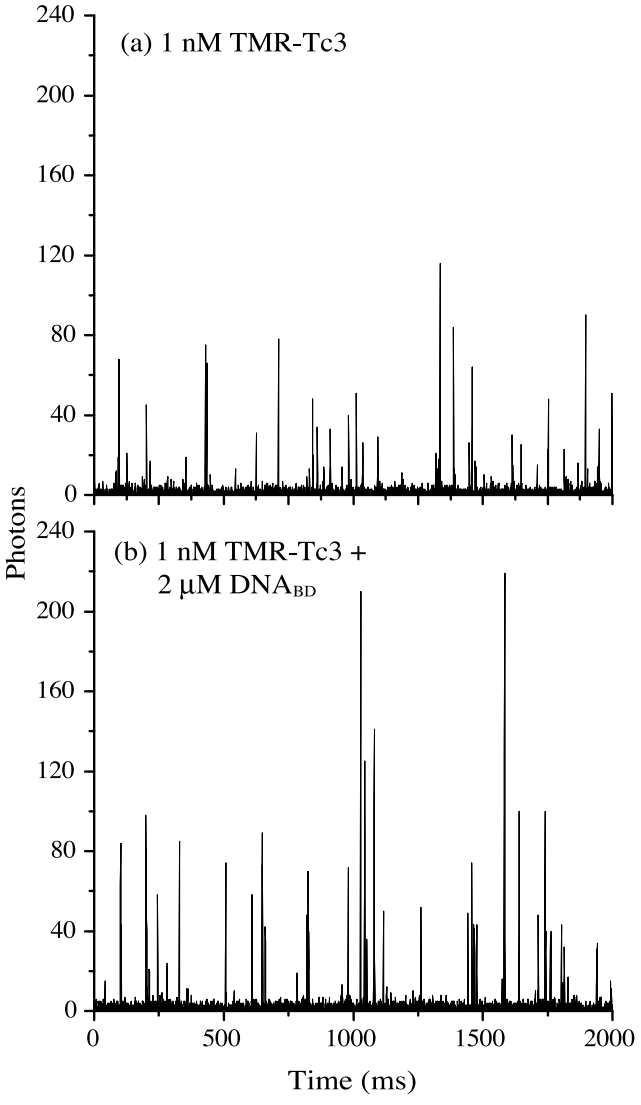

FIGURE 7 MCS data for (*a*) 1 nM TMR-Tc3; (*b*) 1 nM TMR-Tc3 + 2 μM DNA_{BD}. Data were acquired with 1-ms integration intervals.

0.18, and the probe volume is unoccupied most of the time (83%) and contains one and two analyte molecules 15% and 1% of the time, respectively.

Fig. 6 shows typical MCS scans for TMR in water at nominal concentrations of 10^{-9} and 10^{-10} M (concentrations based on absorbance data). The data was acquired at a rate of 1000 points/s (1-ms integration). At 1 nM concentration the detection volume is frequently occupied by more than one molecule. An order of magnitude dilution results in an empty probe volume most of the time, and, as a result, clearly separated bursts of fluorescence are evident. Each burst of fluorescence is due to a single molecule transit through the detection volume. Fig. 7 *a* shows a characteristic MCS trace of 1 nM TMR-Tc3 conjugate in buffer. When compared with Fig. 6 *b* it is immediately evident that many more bursts are recorded for the solution of free TMR

TABLE 1 Burst statistics for solutions of 1 nM TMR-Tc3 (TP^{free}) and 1 nM TMR-Tc3 with 2 μM DNA_{BD} (TP^{bound})

Sample	C_{min}	# Bursts	PD	K_{QF} or K_{QF}^{bound}	τ_R^{exp} (ms)
TP^{free}	8	4497	22	0.092	143
TP^{free}	10	3623	25	0.086	114
TP^{free}	15	2508	32	0.084	138
TP^{bound}	8	4250	32	0.13	134
TP^{bound}	10	3266	38	0.11	119
TP^{bound}	15	2407	50	0.12	137

Data for accumulated 163.8 s of MCS data with 1 ms integration bins. C_{min} is the minimum counts in one bin needed to for a burst to be registered, and PD is the photon density, determined by averaging the (counts)/(ms integration) over the total number of detected events. τ_R^{exp} is the experimentally measured recurrence time.

relative to TMR-Tc3 at the same concentration of TMR and for otherwise identical conditions. Both scans were obtained with 1-ms resolution. The concentrations of both free TMR and TMR-Tc3 were ascertained by absorbance measurements in methanol solvent. The extinction coefficient of TMR in methanol (91,000 cm^{-1} M^{-1} at 544 nm) was also used for the protein conjugate at its peak absorbance, which was red-shifted to 552 nm.

Shown in Fig. 7 *b* is a representative MCS scan acquired from 1 nM TMR-Tc3 with the addition of approximately 2 μM of DNA_{BD}. The mixture of peptide and oligonucleotide was incubated for an hour to establish binding equilibrium before measurements were acquired. In agreement with the bulk-phase fluorescence data, it was discovered that the addition of DNA_{BD} to TMR-Tc3 caused an increase in integrated fluorescence intensity. This effect may be visualized in a qualitative sense through comparison of Fig. 7 *a* and *b*. The magnitude of this result was computed by summing the amplitudes of each MCS bin for the dye-protein system without DNA_{BD} and subtracting the background signal (integrated solvent scans) to obtain the total integrated fluorescence signal. The same procedure was applied to the solution containing TMR-Tc3 and DNA_{BD}. Computed in this manner, it was found that the total fluorescence amplitude of TMR-Tc3 conjugate increased by threefold with the addition of the DNA_{BD}. Although the magnitude differs slightly from the bulk measured value, the result is in qualitative agreement.

Table 1 compares the number of detected events (bursts) and burst widths for 1 nM solutions of the labeled protein both with and without the addition DNA_{BD}. The values are calculated from an accumulated 163.8 s of MCS data with 1-ms integration bins. Deciding exactly what constitutes a burst as opposed to noise unfortunately involves assigning a somewhat arbitrary threshold. Nonetheless, a reasonable threshold may be arrived at by considering the amplitude of the background intensity from solvent only scans. The data shown in the table also show to some degree how the choice of

threshold conditions effects the burst statistics. As indicated in the table, three different threshold conditions were used for each data set. The threshold is indicated by C_{min}, which is the minimum number of counts/millisecond required for a burst to be counted. It is evident that although the threshold criteria affects the total number of bursts counted, the relative statistical differences between data with and without DNA_{BD} is consistent at each threshold level. There are two key results that may be derived from this burst analysis. First, the number of events recorded for the solution of protein alone is ~4 to 10% higher than the number of detected bursts for protein/DNA under otherwise identical conditions, thus the increase in fluorescence upon binding is not due to an increased number of fluorescent events. However, the average burst width for the mixture of DNA and protein is 30 to 45% greater than the average burst width for the solution of protein only and this presumably plays a role in fluorescence increase upon DNA binding.

The addition of DNA_{BD} should result in more than 95% of the protein being bound to the oligo under equilibrium conditions. Because only the protein is labeled, addition of the DNA should contribute nothing to the observed fluorescence signal in the MCS traces. Assuming for the moment that binding has no effect on the fluorescent properties of the TMR label, one would expect to see fewer single molecule transits through the probe volume in a given amount of time for the mixture of peptide and DNA_{BD} versus the peptide alone. The reasoning behind this presumption is simple. The protein-DNA complex has a greater mass than the protein by itself. A more massive particle generally has a smaller diffusion coefficient than a lighter particle. Consequently, and assuming other factors to be equal, a smaller burst frequency should be evident for the protein-DNA mixture. An initial inspection of the results recorded in Table 1 are seemingly explained by simple diffusion, but a more thorough analysis presented below indicates that diffusion is not the limiting factor in the burst statistics.

ANALYSIS AND DISCUSSION

Protein conformational dynamics

To understand binding interactions between the Tc3 peptide and its DNA binding site, it is useful to first characterize the structure and dynamics of TMR-Tc3 by itself. Towards this goal, a comparison of the MCS data for TMR and TMR-Tc3 (Figs. 6 and 7) is found to be revealing. As mentioned previously, it is generally true that an increase in mass is commensurate with a decrease in diffusivity. Thus, the observation of an increased number of single molecule transits through the probe volume for the free dye, TMR, compared with the protein conjugate, TMR-Tc3, might be explained by the difference in mass. The more massive dye-protein complex should diffuse on a slower timescale, and as a result the recurrence time τ_R, which is the time between one molecule leaving the probe volume and another one entering it, would be greater. However, as shown below, diffusion theory is not quantitatively consistent with this explanation.

The diffusion characteristics of the particular particle being monitored will naturally have an effect on the number of events, the duration of each event, and the time interval between events as recorded in each MCS scan. The diffusion coefficient is given by the Stokes-Einstein equation

$$D = \frac{kT}{f} \tag{4}$$

in which k is the Boltzmann constant, T, is the temperature, and f is known as the frictional coefficient (Tanford, 1961). Assuming a spherical molecule of radius R_0, the frictional coefficient is given by

$$f_0 = 6\pi\eta R_0 \tag{5}$$

in which η is the viscosity of the solution and the subscript denotes a spherical particle. A more sophisticated model that permits deviation from spherical geometry and for the possibility that the particle is associated with some solvent molecules (hydrodynamic particle) expresses the diffusion coefficient as (Tanford, 1961)

$$D = \frac{1}{f_A}\frac{kT}{6\pi\eta}\left[\frac{3M(\bar{v}_2 + \delta_1 v_1^0)}{4\pi N_A}\right]^{-1/3} \tag{6}$$

in which M is the molar mass, N_A is Avogadro's number, and f_A is an asymmetry factor. The asymmetry factor takes into account deviation from spherical geometry by means of the ratio $f_A = f_D/f_0$. The actual frictional coefficient, f_D, pertains to a particle that is ellipsoidal in shape but of the same volume as that of sphere having a radius R_0 and frictional coefficient f_0. The quantities $\bar{v}_2$ and v_1^0 are the partial specific volumes (i.e., $v_i = (\partial V/\partial g_i)_{T,P,g_j}$) of the solvated particle and of the pure solvent respectively. δ_1 is a solvation parameter defined as the number grams of solvent component associated with 1 g of the unsolvated (dry) particle.

The TMR-Tc3 complex is neither a sphere nor an ellipsoid, but Eq. 6 may be used to obtain a reasonable estimate of the range of possible values for the diffusion coefficient. For proteins $\bar{v}_2$ is typically in the range of 0.707 to 0.74 $cm^3\ g^{-1}$ with an average of ~0.72 $cm^3\ g^{-1}$. The partial specific volume of water is ~1.0 $cm^3\ g^{-1}$, and for dilute aqueous buffer the viscosity coefficient is ~1 centipoise (0.01 $g\ s^{-1}\ cm^{-1}$). The asymmetry factor ranges from unity for a perfect sphere to ~1.5 as the shape is distorted to that of a prolate (rod) or oblate (pancake) ellipsoid of revolution. For $f_A = 1.5$ the major axis differs by a factor of 10 for a prolate ellipsoid (1/10, oblate), thus it corresponds to a severe distortion from

TABLE 2 Diffusion coefficients and calculated recurrence times, τ_R^{calc}, for aqueous 1 nM Tc3 as a function of the degree of water association, δ_1, and shape as described by the asymmetry factor f_A.

δ_1	D ($cm^2\ s^{-1}$) $f_A = 1.0$	τ_R^{calc} (ms) $f_A = 1.0$	D ($cm^2\ s^{-1}$) $f_A = 1.5$	τ_R^{calc} (ms) $f_A = 1.5$
0.0	1.8×10^{-6}	0.83	1.2×10^{-6}	1.2
0.5	1.5×10^{-6}	0.99	9.9×10^{-7}	1.5
1.0	1.3×10^{-6}	1.1	8.8×10^{-7}	1.7

See text for details.

spherical geometry. The amount of water associated with proteins, represented by δ_1, is typically in the range of 0.2 to 0.6 g/g. The Insight II software package (MSI Software Products, San Diego, CA) was used to model the structure and degree of water association of Tc3 protein in an aqueous environment. The results provided an estimate of δ_1 equal to ~0.5. The molar mass of TMR-Tc3 is 6223 g/mol. With these parameters inserted into Eq. 6, the diffusion coefficient of TMR-Tc3 was computed over a range of possible geometries and amount of solvation for $T = 20°C$. The results are presented in Table 2, and if compared to literature data from other globular proteins (data not shown), it is seen that D scales with the inverse of the cube root of the mass as predicted from Eq. 6.

If the passage of each molecule through the probe volume is a random event that is independent of the movement of any other molecule, then the process may be described by Poisson statistics. Accordingly, if an event (burst) is recorded at time t then the probability (or number of times, N) of an event happening again at some later time $t + \Delta t$ is given by the following equation (Hamming, 1991).

$$N(\Delta t) = \alpha \exp(-\beta \Delta t) \tag{7}$$

The parameter α is a proportionality constant. The slope of a plot of $\ln(N)$ versus Δt yields the parameter β, which is the characteristic frequency at which events occur. The inverse of β gives the recurrence time, τ_R, which is the average time between events. The relationship between the recurrence time and the diffusion coefficient, D, is

$$\tau_R = (4\pi r_0 D n)^{-1} \tag{8}$$

in which n is the particle density (particles/cm^3), and r_0 is the radius of a spherical volume element (Eigen and Rigler, 1994). In these experiments the detection volume is shaped more like an hourglass than a sphere. However, to facilitate the analysis, this volume was approximated as an effective sphere possessing a volume equal to the actual 3.0 fl volume as measured by FCS. The recurrence time predicted by diffusion theory, τ_R^{calc}, was estimated for a 1 nM aqueous solution of Tc3 by inserting the diffusion coefficients from Table 2 into Eq. 8. The results are shown in the same table. The experimentally measured recurrence time, τ_R^{calc}, for the same solution, was found to be 132 ms and was obtained by plotting $\ln N(\Delta t)$ versus Δt and fitting the data to Eq. 7. The measured value of 132 ms is an average of τ_R's calculated for different threshold conditions (see Table 1). An exactly analogous procedure was applied to the MCS data of free TMR at 0.1 nM concentration with the diffusion constant taken to be $2.8 \times 10^{-6}\ cm^2\ s^{-1}$ as determined from previous studies (Zander et al., 1996). This analysis yielded predicted and measured recurrence times of 5.3 and 50 ms, respectively. The analysis was performed on a more dilute solution for the free dye (0.1 nM) to ensure that the statistics were applied exclusively to single molecule events.

The relative agreement between theory and experiment may be concisely expressed as a ratio of the respective recurrence times, with $R = \tau_R^{calc}/\tau_R^{exp}$. It is expected that R will be less than unity because the calculation of τ_R^{calc} assumes that every molecule that enters the detection volume is counted. However, molecules are only counted if their fluorescence emission exceeds some specific threshold condition. For example, a molecule that enters the edge of the probe volume and exits soon thereafter may not emit enough photons to be considered as an "event." In addition, there is some statistical probability that a molecule will suffer photodestruction after a minimal number of absorption/emission cycles and not emit enough photons to exceed threshold criteria. Nevertheless, it is reasonably assumed that these effects should be of similar magnitude for TMR and TMR-Tc3. The excitation intensity was equal for measurements on both systems, and the detection volumes were presumably equal. However, it should be noted that the effective detection volume depends on the degree of optical saturation with respect to the fluorophore, and this level may differ somewhat for free TMR versus TMR-Tc3. Burst events were recorded in both systems that were an order of magnitude greater than the threshold conditions used here. This indicates that the probability of recording a molecular passage through the detection volume is not significantly greater in one system versus the other. Therefore, it should prove informative to compare the relative magnitudes of R obtained for TMR and TMR-Tc3, but little significance will be attached to their actual magnitudes. Plugging in values for the free TMR (T) and TMR-Tc3 (TP) yielded the result $R_T = 0.11$ and $R_{TP} = 0.0091$, respectively. $\tau_R^{calc} = 1.2$ ms was used in computing R_{TP}. This value is an average of the range of τ_R^{calc} values (0.83–1.7 ms) derived by varying the shape factor and amount of water associated with the protein (Table 2).

Evidently, R_T is an order of magnitude greater than R_{TP}. In other words, even after taking into account the theoretical differences in the diffusion of TMR alone and TMR-Tc3, there are more than 10-fold fewer bursts recorded with the conjugate than the free dye for the same dye concentration.

This suggests that a significant fraction of TMR-Tc3 molecules exist in a quenched state, and the effective concentration of fluorescent species is much less than the nominal value expected from the dye concentration. If one then assumes that the system exists in one of two possible states, a fluorescent state, F, or a quenched state, Q, with equilibrium constant K_{QF}:

$$Q \leftrightarrow F \quad K_{QF} = \frac{\langle N_{TP}^{F} \rangle}{\langle N_{TP}^{Q} \rangle} = \frac{\langle N_{TP}^{F} \rangle}{\langle N_{TP}^{tot} \rangle - \langle N_{TP}^{F} \rangle} = \frac{\langle N_{TP}^{F} \rangle}{\frac{\langle N_{TP}^{tot} \rangle}{\langle N_{T}^{F} \rangle} \langle N_{T}^{F} \rangle - \langle N_{TP}^{F} \rangle} \tag{9}$$

The average number of molecules of the ith species in the probe volume that are in a fluorescent or quenched state are $\langle N_i^F \rangle$ and $\langle N_i^Q \rangle$ respectively, and $\langle N_i^{tot} \rangle$ is the average total number of molecules of the ith species in the detection volume. The average number of fluorescent molecules may be expressed as $N^F = t^F/t^{tot}$, in which t^F and t^{tot} are the total time fluorescence was recorded and the total time of the measurement respectively. Using this relationship, along with the assumption that all TMR molecules exist in a fluorescent state, $N_T^F = N_T^{tot}$, leads to the following.

$$K_{QF} = \frac{\langle N_{TP}^{F} \rangle}{\frac{C_{TP}^{tot}}{C_T} \langle N_T \rangle - \langle N_{TP}^{F} \rangle} = \frac{t_{TP}^{F}}{\frac{C_{TP}^{tot}}{C_T} t_T^F - t_{TP}^F} \tag{10}$$

C_i is the concentration of the ith species. The t^{tot} term drops out of the expression since this value was the same in all measurements. The total time spent in a fluorescent state can be approximated as $t^F = \tau^{ACF} B_i F$, in which B_i is the total number of detected bursts for the ith species and τ^{ACF} is the autocorrelation function decay time, which is roughly equal to the average width of a burst. This leads to

$$K_{QF} = \frac{\tau_{TP}^{ACF} B_{TP} F_{TP}}{\frac{C_{TP}^{tot}}{C_T} \tau_T^{ACF} B_T F_T - \tau_{TP}^{ACF} B_{TP} F_{TP}} \tag{11}$$

Assuming that the fraction of bursts actually detected is equal for both TMR and TMR-Tc3, Eq. 11 simplifies to

$$K_{QF} = \frac{\tau_{TP}^{ACF} B_{TP}}{\frac{C_{TP}^{tot}}{C_T} \tau_T^{ACF} B_T - \tau_{TP}^{ACF} B_{TP}} \tag{12}$$

The advantage of Eq. 12 is that the equilibrium constant may be estimated entirely from experimental parameters. The concentrations are derived from absorbance measurements of the stock solutions, and the number of bursts are obtained by counting the number of events as recorded in the MCS data. Results for 1 nM TMR-Tc3 and 1 nM TMR-Tc3 + 2 μM DNA_{BD} are shown in Table 1. From a 0.10 nM solution of TMR burst counts of 4350, 3722, and 2648 were obtained for threshold conditions of $C_{min} = 8$, 10, and 15, respectively. The decay of the ACF will be defined as the time it takes for the ACF to decrease to $1/e$ its initial amplitude. This procedure permits ACF data from different systems to be compared, despite the lack of a mathematical model. The $1/e$ decay time is frequently used as reference point in kinetic analysis. Applied to FCS data (data not shown) gathered from 0.1 nM TMR and excited with 600 μW, a decay time of $\tau_T^{ACF} = 247$ μs was obtained. Analogously, from 1 nM TMR-Tc3 FCS data, τ_{TP}^{ACF} was found to be 202 μs. Values were derived without normalization of the ACF amplitude. Inserting all of this into Eq. 12 yielded an average $K_{QF} = 0.087$, corresponding to the conjugate existing in a dark state ~90% of the time.

As a check on the validity of these results, the average number of fluorescent molecules was determined from the ACF at zero delay time. From Eq. 2 it was evident that $G(0) = 1 + \langle N^F \rangle^{-1}$. From the ACF data shown in Fig. 5 for 1 nM TMR-Tc3 it was found that $\langle N_{TP}^F \rangle = 0.11$. This leads to an equilibrium constant of $K_{QF} = \langle N_{TP}^F \rangle / \langle N_{TP}^{tot} \rangle = 0.061$ (94% quenched), in which $\langle N_{TP}^{tot} \rangle$ was determined from Poisson statistics. Given the rather different assumptions involved in these estimates, the two approaches give reasonably consistent results.

The change in Gibb's free energy for conformational flipping is related to the equilibrium constant via the relationship $\Delta G_{QF} = -RT \ln K_{QF}$. With K_{QF} equal to 0.087, ΔG_{QF} is determined to be 6.0 kJ/mol at 20°C. Digital calculations of equilibrium constants can only be determined through single molecule measurements and represent another novel use of this technology. Such measurements may have application particularly in complex biological mixtures where bulk measurements of more concentrated systems may be influenced by other molecular interactions. The ΔG_{QF} determined above is of the right order of magnitude for what is typically observed for low barrier isomerization reactions and small-scale protein conformational fluctuations (Branden and Tooze, 1991; Tinoco et al., 1995). In any event, it is clear from the single molecule traces that the TMR-Tc3 exists in at least two conformations, one that is fluorescent and one that is not. This is in contrast to a situation in which conjugation of TMR to Tc3 uniformly quenches the TMR fluorescence by a large factor.

Protein-DNA interactions

Upon binding of the TMR-Tc3 to DNA_{BD}, the total fluorescence increases by a factor of 3 to 4 (integration of the single molecule signals gives 3, whereas the steady-state fluorescence change is a factor of 4). There are two apparent mechanisms that could be operating alone or in conjunction with each other to increase the fluorescence of the conjugate upon binding to DNA. It could be that the equilibrium

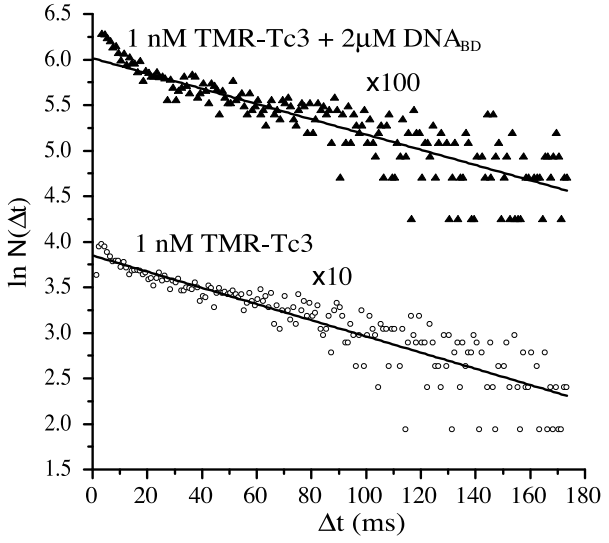

FIGURE 8 Plot of the natural log of the number of times a dark interval occurred ln $N(\Delta t)$ versus the magnitude of the dark interval, Δt for 1 nM TMR-Tc3 (○); 1 nM TMR-Tc3 + 2 μM DNA_{BD} (▲). The solid line is a best fit of Eq. 7 to the data. Data sets are offset for ease of comparison. The threshold condition for registering a burst was triggered if the count rate was ≥10 kHz (C_{min} = 10).

between fluorescent and nonfluorescent forms shifts towards more molecules in the fluorescent form. In addition, there could be a change in the photophysical characteristics of the dye itself resulting in an increased rate of emission. Fig. 8 plots the ln $N(\Delta t)$ versus the time between events, Δt, for 1 nM solutions of TMR-Tc3 both with and without the addition of DNA_{BD}. The line is a least squares fit of Eq. 7 to the data for $\Delta t \geq 6$ ms. Recurrence times are also shown. Surprisingly, the slopes of these two curves are nearly identical, implying that the recurrence times are equivalent for TMR-Tc3 alone and in a solution containing an equilibrium mixture of unbound TMR-Tc3 and TMR-Tc3 bound to DNA_{BD}.

If binding to DNA_{BD} resulted in a fluorescent complex that survived on average longer than the diffusion time one should expect to see a decrease in the recurrence time and also the total number of events, simply because the complex with the DNA should diffuse more slowly. In Table 1, the total number of detected TMR-Tc3 molecules differs only slightly (~4–10%) in the presence of DNA_{BD}. This result implies that some other mechanism besides diffusion regulates the burst frequency.

Additional evidence to support this argument is found in the FCS data. For a diffusion controlled process, the long time component of the ACF decay is determined by the particle's diffusion coefficient and the dimensions of the probe volume. The probe volume dimensions were determined previously from FCS measurements of freely diffusing TMR and R6G. Knowledge of the particle's diffusion coefficient would allow one to calculate the ACF decay time for a process governed purely by diffusion via Eq. 2. This value could subsequently be compared to experiment. An accurate calculation of the diffusion coefficient for a molecule of complex shape like TMR-Tc3 bound to DNA_{BD} is a difficult task. Despite this, a sensible estimate and some reasonable limits may be determined. As a first order approximation the frictional coefficient can be defined in terms of a mass weighted parameter known as the radius of gyration defined as

$$R_g = \left(\sum_i m_i r_i^2 \Big/ \sum_i m_i^{1/2} \right) \tag{13}$$

in which m_i and r_i are the mass and distance from center of mass for ith atom in the complex (Elias, 1977). The software package Insight II was used to artificially construct the DNA_{BD} oligonulcleotide molecule and overlay it with the oligonucleotide structure in the DNA/Tc3 complex obtained from the protein data bank (Fig. 1) (van Pouderoyen et al., 1997). Then the original oligonucleotide from the protein data bank file was deleted, and from this the atomic coordinates were computed. This process was not to obtain an exact structure but rather to produce a structure having the same mass distribution relative to the actual Tc3/DNA_{BD} complex. From these coordinates, R_g was computed to be 31.7 Å and 30.8 Å with and without associated water, respectively. Use of Eqs. 5 and 6 with the approximation $R_0 \approx R_g \approx 31$ Å, it is found that in water D (20°C) is approximately 7×10^{-7} cm^2 s^{-1}.

For comparison, the diffusion constant for a 32-bp (ds)-DNA molecule may be approximated as a rigid cylinder. For ease of calculation, a cylinder of length L and diameter σ may be replaced with a prolate ellipsoid (semiaxes a, b, b) of equal volume. The relationship is between the two geometrical forms is (Tanford, 1961)

$$\frac{\sigma}{L} = \frac{b}{a}\sqrt{\frac{2}{3}} \tag{14}$$

The axis ratio, b/a, is in turn related to the asymmetry factor.

$$f_A = \frac{\sqrt{1 - b^2/a^2}}{(b/a)^{2/3} \ln \dfrac{1 + \sqrt{1 - b^2/a^2}}{b/a}} \tag{15}$$

The length and diameter of a 32-mer (ds- B-form) is 105.6 Å and 23.7 Å, respectively. With these dimensions the diffusion constant is found to be 8.5×10^{-7} cm^2 s^{-1}. By ignoring the additional mass from associated water or bound TMR-Tc3, this value certainly represents an upper limit to the diffusion coefficient of TMR-Tc3/DNA_{BD}.

Fig. 9 plots the experimental ACF obtained from a solution of TMR-Tc3/DNA_{BD} along with the expected curves based on a diffusion-limited process by using the diffusion coefficients estimated above in Eq. 2. The amplitudes are

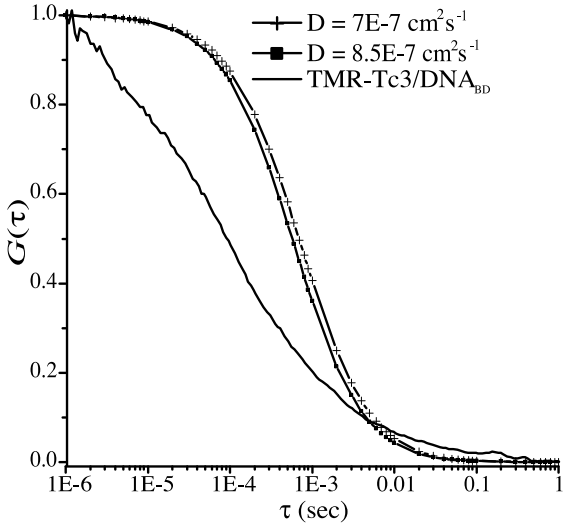

FIGURE 9 Measured ACF for 1 nM TMR-Tc3 with 2 μM DNA_{BD} and theoretical diffusion limited ACF for DNA_{BD} ($D = 8.5 \times 10^{-7}$ cm^2 s^{-1}) and Tc3/DNA_{BD} complex ($D = 7 \times 10^{-7}$ cm^2 s^{-1}). Amplitudes normalized to one. See text for details.

normalized to unity for comparison. It is plainly evident that the observed rate of decay of the experimental ACF is significantly greater than that predicted from diffusion theory, which again supports the conclusion that the burst statistics are not governed by diffusion alone.

What then is the physical process that gives rise to the burst statistics observed here? The data suggest that the rate of interconversion between quenched and fluorescent forms of TMR-Tc3 determines the number and duration of burst events. At 1 nM concentration of TMR-Tc3, the probe volume is occupied by at least one molecule 80% of the time. But only occasionally does the TMR label actually light up and register a signal. Alone in solution, TMR-Tc3 alternates between a quenched and fluorescent state, although the most stable conformation is the quenched form. When bound to DNA_{BD} this conformational flipping still occurs, and it is still true that the TMR is quenched much of the time. However, when TMR-Tc3 does "turn on" it remains fluorescent for a longer time relative to the unbound form. Accurate determination of average burst widths could not be obtained directly from MCS data as it was acquired with only 1-ms resolution. However, the average burst duration for bound TMR-Tc3 is clearly greater than that for the unbound form as evidenced by the longer decay of the autocorrelation function (Fig. 5). Another factor that contributes to the fluorescence increase upon binding to DNA is that the photodynamics of the fluorophore itself changes. Binding results in an increase in the emission rate of the TMR label as seen in Table 1 under the PD (photon density) column.

The equilibrium constant for the interconversion between the quenched and fluorescent forms of the bound TMR-Tc3, K_{QF}^{bound}, may be computed using an analogous procedure as described previously for the calculation of K_{QF} for TMR-Tc3. The prime in Eq. 16 is used to indicate that the fluorescent and quenched forms of the bound and unbound forms are not necessarily identical.

$$K_{QF}^{bound} = \frac{\langle DNA_{BD}{:}F' \rangle}{\langle DNA_{BD}{:}Q' \rangle} \tag{16}$$

The outcome of this calculation yields $K_{QF}^{bound} \approx 0.12$ and $\Delta G_{QF}^{bound} = 5.2$ kJ/mol (Table 1). The equilibrium constant calculated from bulk phase spectroscopy for binding of TMR-Tc3 to DNA ($K_D = 86$ nM) leads to a $\Delta G_{binding} \approx -40$ kJ/mol. This value is relatively large in relation to $\Delta G_{QF}^{bound} = 5.2$ kJ/mol. Thus, the binding energy of the protein is predominantly used for the specific and nonspecific forces that hold the protein in the correct location, and only a small fraction is devoted to altering protein conformation. The increase in equilibrium constant for formation of the fluorescent form roughly accounts for a 40% increase in steady-state fluorescence upon DNA binding. In addition, the average rate of photon emission for bound TMR-Tc3 is ~50% greater relative to the unbound form (Table 1). The fact that the measured increases in these two parameters does not completely account for the three- to fourfold increase in total fluorescence observed presumably has to do with the fact that the single molecule measurements really only consider fluorescent events that are above a certain threshold and limiting constraints on smaller fluorescent events, which are included in the total fluorescence, may be different.

If the signal widths are primarily determined by the rate of conformational interconversion, as opposed to diffusion, then the average time spent in the fluorescent state is approximately equal to the average burst width from the MCS data. Thus for free TMR-Tc3 the fluorescent conformation exists on average for approximately 202 μs and survives slightly longer, ~297 μs (1/e decay of ACF), when bound to DNA_{BD}. Also recall that for the concentrations considered here, there is on average at least one molecule within the detection volume. Thus, this approach results not only in estimates of the equilibrium constant between the fluorescent and nonfluorescent form, but of the times in each state as well.

Finally, the possibility that photochemical production of dark states of the TMR label had some role in the results observed here was considered. Fig. 10 shows normalized ACFs for 1 nM TMR-Tc3 at 400 and 600 μW excitation. It is evident that in both cases the ACF has the same decay, which indicates that photobleaching does not contribute substantially to the processes observed in this study. The extra noise in the ACF decay at 400 μW excitation is attributed to a lower signal to noise relative to the data for 600 μW excitation, which was closer to the saturation level for the dye label.

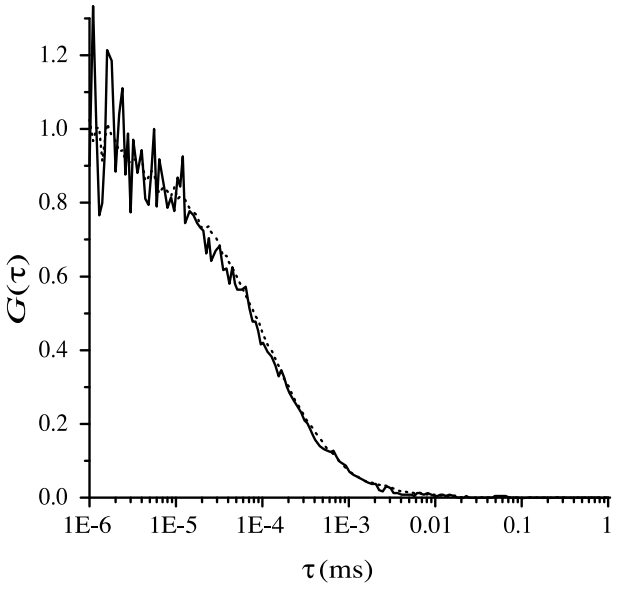

FIGURE 10 Measured ACF for 1 nM TMR-Tc3 at 400 μW (*solid*) and 600 μW (*dashed*) excitation power. ACF amplitudes are normalized to an amplitude of unity.

SUMMARY

Fluorescence measurements at the single molecule level indicate that a significant percentage (90%) of the labeled protein, TMR-Tc3, exists in one or more conformations that quench TMR fluorescence. Whether bound or unbound to its consensus DNA sequence, TMR-Tc3 spends most of its time in the quenched state, but when bound, it remains in a fluorescent state for longer relative to the unbound form. The rate of emission also differs between the bound and unbound form implying that the two fluorescent conformations (bound and unbound) are not identical. Protein binding to nucleic acid structures is frequently depicted as effecting static structural changes. The commonly portrayed modus operandi is one in which the free protein exists in one form prior to binding, and upon attachment to DNA, subsequently converts to a different structure and remains in that configuration until dissociation. Contrary to this scenario, the data here paints a picture of the bound protein as not locked into one particular form, but instead fluctuating between one or more conformations. Binding to DNA merely changes the statistical probability of being in one form or another. It is not known for sure whether the conformational changes are local to the TMR or more global in nature. However, the observation that fluorescence is substantially affected upon binding of TMR-Tc3 to DNA_{BD} suggests that long range structural changes play a significant role in the fluorescence properties of the complex. In any event, probing individual molecules opens the door to investigating these mechanistic details that are largely unavailable in bulk phase experiments.

REFERENCES

Bradford, M. M. 1976. A rapid and sensitive method for the quantitation of microgram quantities of protein utilizing the principle of protein-dye binding. *Anal. Biochem.* 72:248–254.

Branden, C., and J. Tooze. 1991. Introduction to Protein Structure. Garland Publishing, Inc., New York and London.

Burley, S. K. 1996. The TATA box binding protein. *Curr. Opin. Cell. Biol.* 6:69–75.

Daniel, D. C., M. Thompson, and N. W. Woodbury. 2000. Fluorescence intensity fluctuations of individual labeled DNA fragments and a DNA binding protein in solution at the single molecule level: a comparison of photobleaching, diffusion, and binding dynamics. *J. Phys. Chem.* 104: 1382–1390.

Deniz, A. A., T. A. Laurence, G. S. Beligere, M. Dahan, A. B. Martin, D. S. Chemla, P. E. Dawson, and S. Weiss. 2000. Single-molecule protein folding: diffusion fluorescence resonance energy transfer studies of the denaturation of chymotrypsin inhibitor 2. *Proc. Natl. Acad. Sci. U.S.A.* 97:5179–5184.

Eggeling, C., S. Berger, L. Brand, J. R. Fries, J. Schaffer, A. Volkmer, and C. A. M. Seidel. 2001. Data registration and selective single-molecule detection analysis using multi-parameter fluorescence detection. *J. Biotechnol.* 86:163–180.

Eggeling, C., J. R. Fries, L. Brand, R. Günther, and C. A. M. Seidel. 1998. Monitoring conformational dynamics of a single molecule by selective fluorescence spectroscopy. *Proc. Natl. Acad. Sci. U.S.A.* 95:1556–1561.

Eigen, M. and R. Rigler. 1994. Sorting single molecules: application to diagnostics and evolutionary biotechnology. *Proc. Natl. Acad. Sci. U.S.A.* 91:5740–5747.

Elias, H.-G. 1977. Macromolecules. Stratford JW, translator. Plenum Press, New York.

Ha, T., T. A. Laurence, D. S. Chemla, and S. Weiss. 1999a. Polarization spectroscopy of single fluorescent molecules. *J. Phys. Chem. B.* 103: 6839–6850.

Ha, T., A. Y. Ting, J. Liang, A. A. Deniz, D. S. Chemla, P. G. Schultz, and S. Weiss. 1999b. Temporal fluctuations of fluorescence resonance energy transfer betwween two dyes conjugated to a single protein. *Chem. Phys.* 247:107–118.

Hamming, R. W. 1991. The art of probability: for scientists and engineers. Addison-Wesley Publishing, Inc., Reading, Mass.

Jäger, J. and J. D. Pata. 1999. Getting a grip: polymerases and their substrate complexes. *Curr. Opin. Struc. Biol.* 9:21–28.

Kingman, J. F. C. 1993. Poisson Processes. L. C. G. Rogers, editor. Clarendon Press, New York.

Krajewska, W. M. 1992. Regulation of transcription in eukaryotes by DNA-binding proteins. *Int. J. Biochem.* 24:1885–1898.

Lu, P. H. and X. S. Xie. 1997. Single molecule kinetics of interfacial electron transfer. *J. Phys. Chem. B.* 101:2753–2757.

Rigler, R., Ü. Mets, J. Widegren, and P. Kask. 1993. Fluorescence correlation spectroscopy with high count rate and low background: analyisis of translational diffusion. *Eur. Biophys. J.* 22:169–175.

Schildbach, J. F., A. W. Karzai, B. E. Raumann, and R. T. Sauer. 1999. Origins of DNA-binding specificity: role of protein contacts with the DNA backbone. *Proc. Natl. Acad. Sci. U.S.A.* 96:811–817.

Soultanas, P., M. S. Dillingham, F. Papadopoulos, S. E. V. Phillips, C. D. Thomas, and D. B. Wigley. 1999. Plasmid replication initiator protein RepD increases the processivity of PcrA DNA helicase. *Nucleic Acids Res.* 27:1421–1428.

Tanford, C. 1961. Physical Chemistry of Macromolecules. John Wiley & Sons, Inc., New York.

Thompson, M. and N. W. Woodbury. 2000. Fluorescent and photochemical properties of a single zinc finger conjugated to a fluorescent DNA-binding probe. *Biochemistry.* 39:4327–4338.

Tinoco, I., Jr., K. Sauer, and J. C. Wang. 1995. Physical Chemistry: Principles and Applications in Biological Sciences. Prentice-Hall, Inc., New Jersey.

Vámosi, G., C. Gohlke, and R. M. Clegg. 1996. Fluorescence characteristics of 5-carboxytetramethylrhodamine linked covalently to the 5′ end of oligonucleotides: multiple conformers of single-stranded and double stranded dye-DNA complexes. *Biophys. J.* 71:972–994.

van Pouderoyen, G., R. F. Ketting, A. Paerrakis, R. H. Plasterk, and T. K. Sixma. 1997. Crystal structure of the specific DNA-binding domain of Tc3 transposase of *C. elegans* in complex with transposon. *EMBO J.* 16:6044–6054.

Walther, A. P., X. V. Gomes, Y. Lao, G. C. Lee, and M. S. Wold. 1999. Replication protein A interactions with DNA: 1. Functions of the DNA-binding and zinc-finger domains of the 70 kDa subunit. *Biochemistry.* 38:3963–3973.

Zander, C., M. Sauer, K. H. Drexhage, D. S. Ko, A. Schultz, J. Wolfrum, L. Brand, and C. Eggeling. 1996. Detection and characterization of single molecules in aqueous solution. *Appl. Phys. B.* 63:517–523.